Cold Pools and MCS Propagation: Forecasting the Motion of Downwind-Developing MCSs

STEPHEN F. CORFIDI

NOAA/NWS/NCEP/Storm Prediction Center, Norman, Oklahoma

(Manuscript received 13 March 2003, in final form 20 May 2003)

ABSTRACT

The primary factors that affect the direction of propagation and overall movement of surface-based mesoscale convective systems (MCSs) are discussed. It is shown that although propagation is indeed related to the strength and direction of the low-level jet as previous studies have shown, it is more specifically dependent upon the degree of cold-pool-relative flow and to the distribution of conditional instability present along a system's gust front. An updated technique that may be used to forecast the short-term (3–6 h) motion of MCS centroids based on these concepts is introduced. The procedure builds on the long-established observation that MCS motion is a function of 1) the advection of existing cells by the mean wind and 2) the propagation of new convection relative to existing storms. Observed wind and thermodynamic data, in conjunction with anticipated cold-pool motion and orientation, are used to assess the speed and direction of cell propagation, that is, whether propagation will be upwind, downwind, or some combination of the two. The technique ultimately yields an estimate of overall system movement and has application regardless of scale, season, or synoptic regime.

1. Introduction

Thunderstorms are frequently organized in lines or clusters known as mesoscale convective systems (MCSs). The term MCS is generally reserved for ensembles of storms that satisfy certain spatial or temporal criteria (see, e.g., Houze 1993, p. 334; Parker and Johnson 2000). In a less restrictive sense, however, any mesoalpha- or mesobeta-scale (Orlanski 1975) area of moist convection might be considered an MCS (Ray 1990).

Because MCSs produce a disproportionate share of significant convective weather (high winds, flash flooding, etc.) and because their evolution is often not predicted well by operational numerical guidance, forecasting MCS motion is of considerable importance to operational meteorologists. Forecasts of MCS motion are dependent upon anticipation of the predominant propagational mode or modes likely during an event. In particular, it is important to distinguish between MCS environments conducive to upwind propagation and those that exhibit downwind storm development and sometimes evolve into derecho-producing squall lines.

Attempts to forecast MCS movement have met with mixed results. Merritt and Fritsch (1984) examined the motion of more than 100 MCSs, most of which were mesoscale convective complexes (MCCs; Maddox 1980). They were among the first to recognize that though no true ''steering level'' exists for MCC motion, such systems typically move approximately parallel to the contours of the 1000–500-hPa thickness. They also noted that although most convective systems move downshear along the contours, others inexplicably move upshear. The speed of MCC motion was found to be modulated by the location of maximum low-level moisture convergence relative to existing convection.

Newton and Katz (1958) and Chappell (1986), among others, showed that the motion of a convective system can be thought of as being the vector sum of 1) an advective component approximated by the direction and magnitude of the mean cloud-layer wind and 2) a propagation component governed by the rate and location of new cell formation relative to existing convection. Building on this idea, and extending the work of Merritt and Fritsch, Corfidi et al. (1996) showed that the propagation component is, in many cases, directly proportional but opposite in direction to the low-level jet. This finding is somewhat surprising given that MCS propagation can be influenced by a myriad of factors such as the distribution of convective available potential energy (CAPE), convective inhibition, gravity waves, outflow boundaries, and orographic effects.

This paper discusses MCS motion, with emphasis on those factors related to a system's cold pool that most influence cell propagation and, ultimately, overall system movement. Based on this presentation, a vector-based forecast technique is developed for predicting the

Corresponding author address: Stephen F. Corfidi, Storm Prediction Center, 1313 Halley Circle, Norman, OK 73069.
E-mail: stephen.corfidi@noaa.gov

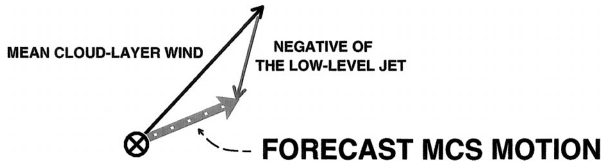

FIG. 1. Schematic of the original vector technique, with MCS core motion (thick dotted arrow) expressed as the vector sum of 1) advection of cells by the mean cloud-layer wind (arrow pointing to upper right) and 2) cell propagation directed into the low-level jet (arrow pointing to bottom of page). MCS centroid is depicted by the cross symbol (after Corfidi et al. 1996).

motion of MCSs characterized by downwind propagation.

2. Background

a. The original vector technique

Corfidi et al. (1996) developed a simple technique to predict the short-term (3–6 h) motion of the mesobeta-scale cores or ''centroids'' of MCSs using the low-level jet to estimate the direction and rate of storm propagation. Forecast centroid motion is taken to be the sum of 1) a vector that represents cell advection by the mean cloud-layer wind (with ''cloud layer'' taken to be the 850–300-hPa layer)[1] and 2) a vector that represents storm propagation, that is, new cell development, equal in magnitude but directed opposite to the low-level jet (Fig. 1). In practice, the 850-hPa wind is used to approximate the low-level jet, although it is recognized that this approach may not identify the true jet in all cases. In the absence of a distinct low-level speed maximum in the vertical direction, the strongest wind in the lowest 5000 ft (1.5 km) is generally used, in accordance with Bonner (1968).

The vector technique is applicable in any kind of environmental wind regime and requires knowledge of only the 850-hPa and mean cloud-layer winds. The procedure is especially useful in identifying those kinematic situations conducive to the development of quasi-stationary and ''back building'' MCSs (Bluestein and Jain 1985). Quasi-stationary systems arise when the wind profile is unidirectional and cell advection is exactly offset by cell propagation. Back building occurs under similar conditions but when propagation exceeds advection, resulting in overall upwind motion. Identification of such events is important because they frequently are associated with excessive rainfall (Chappell 1986).

The original vector concept, while useful, is nevertheless subject to several limitations. First, the scheme does not account for spatial and temporal changes in the environmental wind that, in altering both cell advection and propagation, can affect MCS movement. Therefore, motion estimates must be updated frequently when the wind field exhibits significant spatial or temporal variability. Second, there is no accounting for the influence of terrain on convective development and low-level flow. As a result, the concept is more difficult to apply in cases of orographically forced convection (e.g., Pontrelli et al. 1999).

A more serious shortcoming of the original vector approach follows from its assumption that new cell development and, therefore, system propagation always occur in the direction opposite that of the low-level jet, or, more generally, the low-level flow. To be sure, many warm-season MCSs over the central United States indeed do exhibit propagation in that direction (see, e.g., Moore et al. 1993; and Junker et al. 1999) at a rate approximated by the speed of the jet.[2] It is clear, however, that this is not always the case. For example, derecho-producing squall lines often move at a substantial angle to the low-level flow, especially during their initiation (Johns et al. 1990). Radar data reveal that, although propagation is largely responsible for the observed motion of these systems, new cell development is not necessarily directed into the low-level flow but rather occurs on the leading (downwind) edge of the system cold pool. For this reason, to be more universally applicable, the vector concept must be modified to account for the presence of cold pools and the potential for propagation away from the low-level flow.

b. Cold-pool and gust-front motion

One of the more distinctive features of a well-organized MCS is the cold pool that develops at lower levels beneath or just behind the strongest convection. Cold pools represent the collective outflow of individual convective cells and the negative buoyancy of parcels within or beneath the convection. Sublimation and/or melting and evaporation of precipitation falling through unsaturated air, precipitation drag, and vertical perturbation pressure gradients are all factors that may enhance downdraft development and cold-pool strength.

The periphery of a cold pool, that is, the gust front or outflow boundary, is marked by low-level convergence and ascent (Purdom 1973; Charba 1974; Goff 1976). As a result, gust fronts are often the site of new cell development. Such activity typically is not distributed evenly along such boundaries. Instead, storm initiation tends to occur in discrete zones, within which kinematic and/or thermodynamic factors are most favorable for development. Observation suggests that *new cell development occurs most readily where the ambient,*

[1] The speed and direction of the mean cloud-layer wind are calculated using the following relationship: Vmean = (V850 + V700 + V500 + V300)/4, where V850 is the 850-hPa vector wind, etc.

[2] The original dataset used by Corfidi et al. (1996) was composed primarily of nocturnal MCCs that were associated with well-defined low-level jets east of the Rockies. In retrospect, therefore, it is not surprising that propagation was found to be correlated well with the low-level jet.

low-level inflow relative to the boundary is greatest. This result follows because areas of strong relative inflow will also be regions of maximum lower tropospheric convergence. As previously noted, these regions are often governed by the position of the low-level jet. If a significant degree of relative motion exists between a gust front and the low-level environmental wind, however, convergence maxima may develop along the boundary in locations away from the low-level jet.

It is obvious that motion of a gust front must be known if the pattern and intensity of relative inflow along it are to be assessed. Many studies (see, e.g., Charba 1974; Goff 1976; Wakimoto 1982; Droegemeier and Wilhelmson 1987; Rotunno et al. 1988) have examined the motion of gust fronts. These investigations determined that storm outflow behaves more or less as a gravity current. Indeed, observational studies (e.g., Wakimoto 1982) have confirmed that downstream gust-front speed is governed largely by the density difference between the downdraft air and that of the surrounding environment and by the depth of the outflow. Because evaporative cooling and precipitation drag often vary markedly over time and space, however, downdraft production is both temporally and spatially unsteady. In addition, cold-pool depth and horizontal density differences ordinarily cannot be measured in real time. For these reasons, gravity-current theory has proven to be of limited operational value in forecasting gust-front motion.

Given the limited utility of gravity-current theory, it is worthwhile to consider the role of momentum transfer in determining gust-front motion, because lower-tropospheric wind data are generally readily available in an operational setting. It is clear that, because of momentum transfer, a gust front will move preferentially in the direction of the motion associated with the parcels that contributed to the parent cold pool. Momentum transfer largely explains, for example, why derecho-producing MCSs embedded in northwesterly midtropospheric flow typically move southeastward (Johns and Hirt 1987). The systems move southeast because their gust fronts advance primarily in that direction. With boundary layer convergence maximized along the gust front on the southeast (downwind) side of the cold pools, new cell development and, therefore, overall system motion are toward the southeast (assuming the existence of a favorable thermodynamic environment).

Perhaps more surprising is that observation suggests that momentum transfer may also be used to estimate gust-front speed. Many processes, of course, can influence gust-front motion on the local (i.e., mesogamma) scale. Because these processes are often nonlinear, gust-front speed is typically unsteady over periods on the order of tens of minutes. Over longer intervals, however, downwind gust-front behavior is observed to be more uniform (e.g., Fovell and Ogura 1989). In fact, subjective examination of nearly 50 forward-propagating MCSs over the central and eastern United States during the last two decades has determined that, at least to a first approximation, *average downwind gust-front speed may be estimated by the mean cloud-layer wind or, more specific, the speed of the parcels that contribute to the parent cold pool.* As will be shown in later sections, this finding may be used to help to estimate the motion of a forward-propagating MCS.

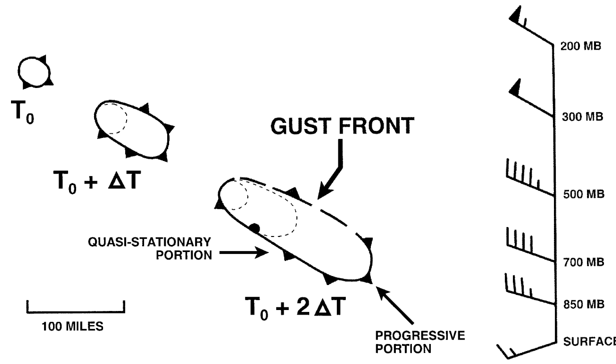

FIG. 2. Plan-view schematic depicting temporal elongation of a cold pool and gust front associated with the hypothetical quasi-unidirectional wind profile shown at right. Motion of boundary relative to ground is depicted by conventional frontal symbols. Dashed lines indicate gust-front positions at earlier times. Indicated spatial scale is for illustrative purposes only.

c. The role of gust-front orientation

Implicit in the observation that cold-pool motion is determined to a large extent by momentum transfer is the fact that, over time, *cold pools tend to elongate in the direction of the mean wind.* This tendency is most pronounced when the flow is unidirectional. As a cold pool elongates, some parts of its associated gust front necessarily become oriented perpendicular to the mean wind while other portions come to lie parallel to it. Continued production of storm outflow forces boundary segments oriented perpendicular to the mean wind to progress downwind with time while flow-parallel portions move very slowly or not at all (Fig. 2).

The orientation of a gust front relative to the mean wind is important in determining the direction of cell propagation and, therefore, the kind of MCS that will be most favored along it. For example, if sufficient surface-based instability is present along those segments aligned parallel to the mean flow, new storm development is likely to occur repeatedly where low-level convergence along the boundary is greatest. This, of course, is often in the direction of the low-level jet. In a typical situation, a component of the propagation will be upwind relative to the mean flow. As a result, cells subsequently track downwind in succession (''train'') along the front (Fig. 3, top). Because the boundary does not move, extended periods of such upwind development can yield excessive precipitation as long as the wind profile remains unchanged. Indeed, this scenario de-

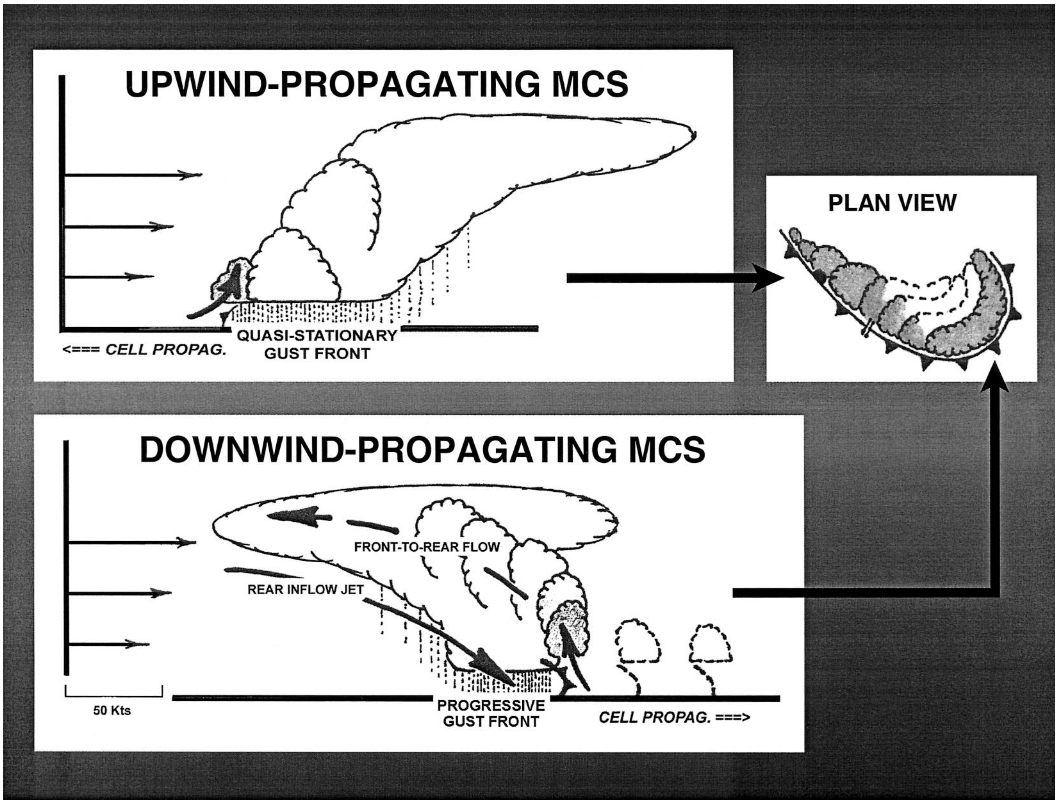

FIG. 3. (right) Plan view of an elongating cold pool, with cross sections perpendicular to the gust front along (top) a quasi-stationary segment and (bottom) a progressive segment, showing direction of cell propagation. Hypothetical wind profiles at left are for illustrative purposes only.

scribes the ''mesohigh'' flash-flood MCS pattern of Maddox et al. (1979).

If instability is present along those portions of the gust front oriented perpendicular to the mean wind, thermodynamics are favorable for the formation of strong convective-scale downdrafts, and sufficient convergence is present to initiate storms, downwind or ''forward'' propagation is likely to occur. Assuming that these conditions are maintained for some period of time, a bow echo or derecho-producing MCS may develop (Fig. 3, bottom). Because cell advection and propagation are additive, some degree of front-to-rear flow will necessarily be present relative to the gust front. Such systems occasionally move much faster than the mean wind when the propagation rate is great.

d. Concurrent upwind and downwind propagation

The role of gust-front orientation in determining propagation direction and MCS type is perhaps best demonstrated by the occasional observation of concurrent back-building and forward-propagating convective systems in environments of largely unidirectional mean flow and minimal cloud-layer shear. As Chappell (1986) noted, environments that are kinematically supportive of quasi-stationary or back-building MCSs may also yield fast-moving, forward-propagating squall lines. Indeed, the implied wind profile in Maddox et al.'s (1979) schematic depicting a back-building ''synoptic'' flash-flood-producing MCS (their Fig. 6) is similar to that found by Johns et al. (1990) to be associated with derecho-producing squall lines (their Figs. 4–8). What distinguishes between the two propagational modes is the orientation of the gust front relative to the mean wind.

The radar evolution of two concurrent bow echo/back-building MCS events is depicted in Fig. 4. The first occurred in moderate westerly flow on the northern edge of a subtropical ridge on 24 August 1998 (Fig. 4a). A small bow-shaped MCS moved across northern Illinois and Indiana, producing wind gusts to 80 kt (40.0 m s^{-1}) near Chicago, Illinois. The bow MCS was followed by a back-building convective cluster that subsequently caused heavy rain over neighboring parts of northern Illinois. The latter system developed along and just behind the trailing outflow boundary (gust front) associated with the bow MCS as the boundary became quasi-stationary and parallel to the westerly unidirectional mean wind.

A similar event affected the Kansas City, Missouri, area several weeks later (Fig. 4b). Thunderstorms de-

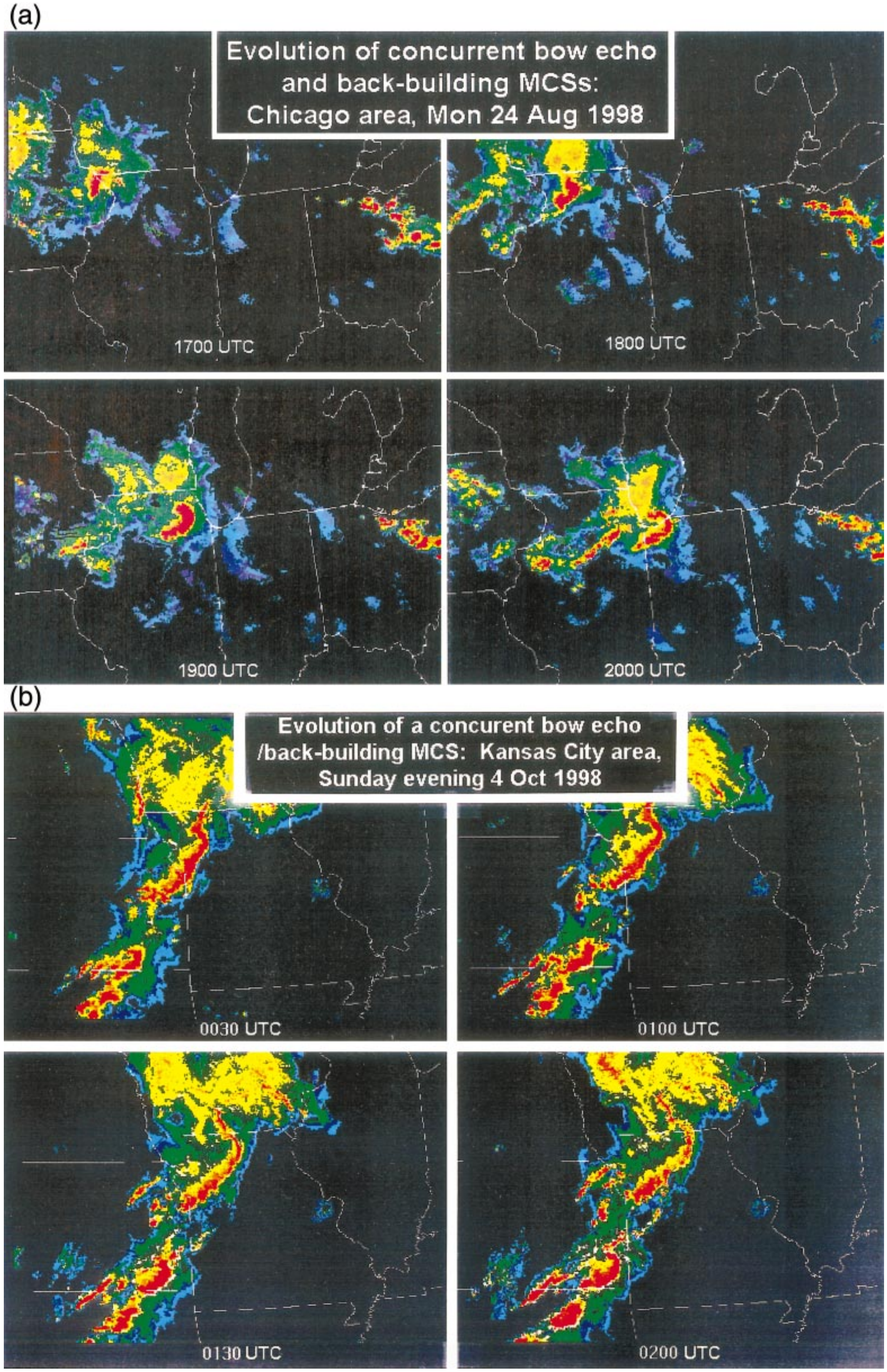

FIG. 4. Composite Doppler radar depiction of reflectivity over (a) northern Illinois, 1700–2000 UTC 24 Aug 1998 and (b) northern Missouri, 0030–0200 UTC 5 Oct 1998.

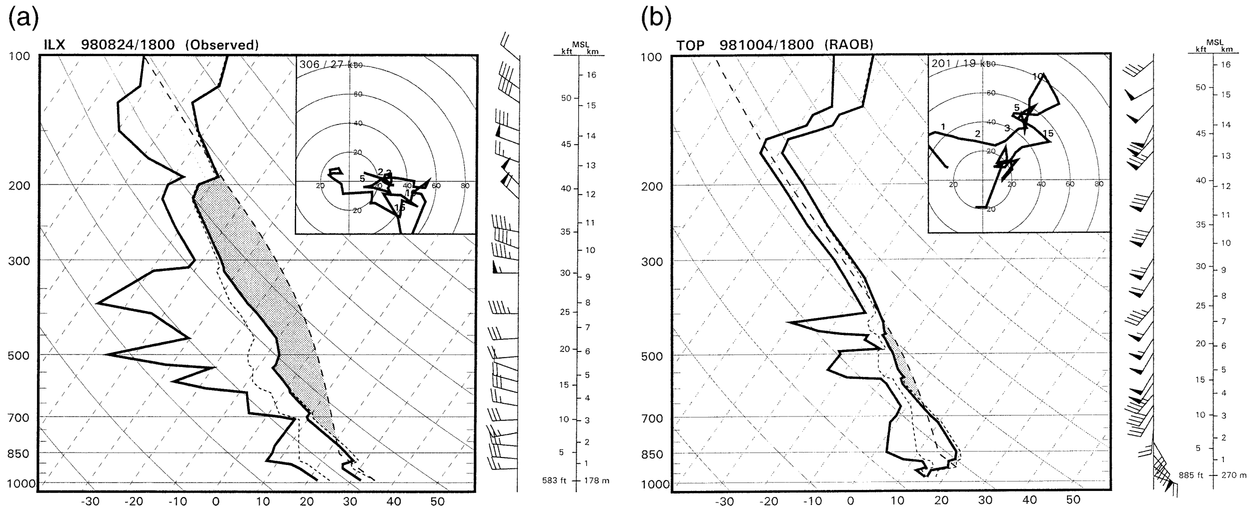

FIG. 5. Skew *T*–log*p* plot of radiosonde observations for (a) Lincoln, IL (near Springfield), at 1800 UTC 24 Aug 1998, and (b) Topeka, KS, at 1800 UTC 4 Oct 1998. Winds are in knots [barb = 10 kt (5 m s^{-1}); flag = 50 kt (25 m s^{-1})]. Lifted parcel ascent curve (large dashed line) is for most unstable parcel, including correction for virtual temperature (rightmost small dashed line). Wet-bulb zero line is shown as a dashed line between environmental temperature and dewpoint profiles. Numbers on the hodograph in the upper-right-hand side depict the altitude above ground level in kilometers.

veloped during the afternoon along a stationary front oriented parallel to a zone of strong unidirectional southwest flow aloft. By evening, the activity evolved into a linear MCS containing an embedded bow echo. The bowed segment of the system produced damaging winds in northern Missouri. Of more significance was the flash flooding in Kansas City that accompanied the trailing southwestern part of the same complex. The flooding occurred as storm cells repeatedly developed and moved northeast along the stalled outflow boundary left by the exiting bow.

The MCS genesis region in both the Illinois and Missouri events was characterized by unidirectional low-to-midtropospheric flow, with limited shear in the cloud-bearing layer [Figs. 5a,b; note that the Topeka, Kansas, sounding (Fig. 5b) was taken just west of the surface front mentioned in the previous paragraph; the portion of sounding above 850 hPa is believed to be representative of warm-sector conditions east of the front]. Similar conditions prevailed farther downstream, along the paths taken by the forward-propagating members of each event. As the cold pools elongated, the gust-front segments oriented perpendicular to the mean wind became the site of downwind convective development while upwind propagation persisted on those portions of the boundary that became quasi stationary.[3]

e. The role of dry air

Previous work has suggested that, in addition to gust-front orientation and motion, thermodynamic factors might also play a role in determining the primary mode of MCS propagation. For example, Corfidi (1998) conducted a preliminary examination of proximity soundings from MCSs that occurred in environments of largely unidirectional flow over the central and eastern United States between 1980 and 1998. The results suggest that a characteristic common to those systems that evolved into bow echoes and/or derechos was the presence of relatively dry air, either at midlevels or in the subcloud layer, ahead of the developing convective system. This air appeared to be associated with the formation of a strong cold pool. In converse, quasi-stationary and back-building MCSs were found to occur in moister or nearly saturated lower-tropospheric environments, with comparatively weak cold pools. In short, the potential to produce cold convective-scale downdrafts (and, therefore, a strong cold pool) appeared to distinguish forward-propagating environments from those more conducive to upwind development.

Dry air is, of course, clearly associated with the occurrence of derechos and bows. Johns et al. (1990) noted the presence of large dewpoint depressions at 700 and 500 hPa in the vicinity of long-lived derechos, and the ingestion of dry air from the prestorm environment can assist in the formation and maintenance of surface mesohighs by enhancing storm-scale buoyant pressure fields and their associated gust-front circulations.

More recent analysis, however, using a dataset of 48 forward-propagating MCSs associated with damaging surface winds, along with examination of quasi-station-

[3] Although not recognized as such at the time, one of the first documented concurrent bow-echo/back-building MCS events was the Independence Day storm of 4–5 July 1969. Widespread damage from high winds followed by flash flooding left 41 dead across Michigan, Ohio, and Lake Erie (Hamilton 1970).

ary systems that produced major flash floods in recent decades, suggests that the relationship between cold-pool strength and forward-propagating MCS development is not so clear. Cold pools are not necessarily weak in all cases of quasi-stationary or back-building convection; indeed, some quasi-stationary MCSs exhibit prominent cold pools. For example, the system that produced the Johnstown, Pennsylvania, flood in July of 1977 (Hoxit et al. 1978; Bosart and Sanders 1981) had a strong cold pool, and a similarly strong cold pool was present in the Kansas City flood case just discussed. Cold-pool strength and, therefore, expansion rate are certainly positively correlated with downwind MCS development, but it is clear that the potential to produce a strong cold pool cannot *alone* be used to distinguish between environments conducive to upwind versus downwind development; gust-front orientation and motion are also important.

3. A vector technique for downwind-propagating MCSs

a. Development of a vector scheme for downwind-developing MCSs

In this section, a scheme similar to that presented in Corfidi et al. (1996) to estimate the short-term motion of forward-propagating MCSs is described. Using the original (1996) technique as a starting point, the approach applies the concepts discussed in the previous section to account for cell propagation away from the low-level jet, along the downwind side of a cold pool.

It has been noted that momentum transfer forces gust-front segments oriented perpendicular to the mean flow to move downwind over time. It has been noted also that the rate of downwind gust-front motion is strongly correlated with the speed of the mean cloud-layer wind. Because the gust front is the mobile locus of new convective development in a forward-propagating MCS, a motion estimate for the boundary (i.e., the cloud-layer wind) can serve as a proxy for the *advective* component of forward-propagating MCS motion.

If one accepts that the advective component of a forward-propagating convective system is given by the mean cloud-layer wind, examination of the schematic depicting the original vector technique (Fig. 1) reveals that the MCS motion vector provided by that scheme is, in fact, the *propagation* vector of a forward-propagating system. This result follows because the motion vector of the original scheme represents the vector difference between a gust front moving at the speed of the mean cloud-layer wind and the low-level flow. In other words, *the motion vector provided by the original technique is, in fact, the negative of the gust-front-relative low-level flow for a boundary moving with the speed and direction of the mean cloud-layer wind.*

The length of the motion vector provided by the original technique is directly proportional to the degree of convergence and rate of new cell development along the gust front. Addition of this vector representing cell propagation along the gust front to that representing the downwind motion of the boundary (i.e., the mean cloud-layer wind) can therefore provide an estimate of the overall motion of a forward-propagating MCS. In short, the vector approach for a forward-propagating system requires just one extra vector addition beyond the two used in the original method (where upwind cell development is assumed) and can yield a drastically different forecast motion, as shown in Fig. 6.

b. Results

Table 1 presents the results of applying the forward-propagating vector technique to 48 convective systems associated with damaging surface winds. The events occurred throughout the central and eastern United States, predominantly during the spring and summer. They were selected on the availability of a sounding representative of the inflow environment [uncontaminated, and within 100 n mi (185 km) and 2 h of the event] and composite radar data. Forecasts were made for the 3-h motion of the strongest MCS radar reflectivity core (the MCS centroid).

As the table shows, successful forecasts [defined as direction and speed of motion within 20° and 10 kt (5.0 m s^{-1}), respectively, of observed] were produced for 38 of the 48 events. On average, the speed errors are random, although there appears to be a tendency to underestimate the forward motion of systems containing embedded supercells and/or strong rear-inflow jets (labeled ''SPRCL/RIJ'' in right-most column of Table 1) Enhanced and/or otherwise altered downstream propagation rates associated with the presence of these features are believed to be responsible for the errors.

The directions of motion forecast by the downwind technique display a small left bias (negative directional errors in Table 1). This observation most likely reflects the large-scale warm-advection environment within which the MCSs occurred. Because the lower-tropospheric shear typically turns right (clockwise) downstream from warm-advection maxima, there is a tendency for forward-propagating MCSs to turn right with time (e.g., Johns et al. 1990). Of course, these systems do not physically change direction per se; the ''turning'' reflects a gradual rightward shift in the area most favored for new cell development as the systems move downwind. Because application of the vector technique uses instantaneous wind data obtained at a given point in time, it is impossible to account for such longer-term rightward deviation in any one forecast. The effect is, however, seen easily if simultaneous forecast motions are plotted spatially on a regional grid. Note also that, for longer-lasting systems, Coriolis accelerations acting on the rear-to-front and front-to-rear flows may also bias motion to the right (Skamarock et al. 1994).

A surface boundary external to the convective system that forced propagation to occur away from the purely downwind direction resulted in significant directional

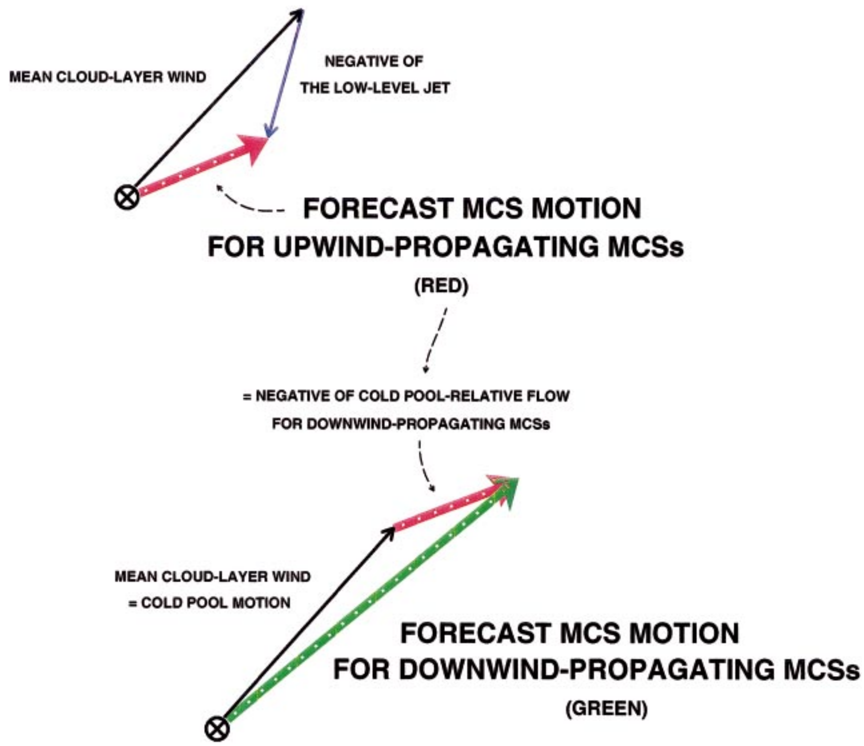

FIG. 6. Comparison schematics of (top) original (upwind) and (bottom) downwind versions of the vector technique to forecast short-term motion of upwind-developing systems (MCS motion given by thick red arrows) and downwind-developing systems (MCS motion given by thick green arrow at bottom of figure), respectively. Vector lengths are proportional to wind speed; MCS centroids are denoted by the cross symbol.

errors in three warm-season cases (11, 32, and 36). It is clear that surface data in the vicinity of a developing MCS must be examined carefully to identify any synoptic or mesoscale boundaries that might have such an effect. Such situations will require modification of the vector technique (namely, rotation of the propagation vector) to account for the altered direction of propagation.

Three of the 10 unsuccessful forecasts in Table 1 appear to have been related to the large-scale environment in which the events occurred. Each was associated with a serial bow MCS along a cold front (Johns and Hirt 1987), and forecast speed was overestimated in each case. In one instance (case 16), overall system motion was slowed because surface-based instability, present both upwind and downwind from the initial convective area, enabled the MCS to exhibit simultaneous upwind and downwind propagation. In the remaining two cases (20 and 29), system motion appeared to be overestimated because propagation was very limited relative to advection. The squall lines moved downstream roughly at the speed of the mean wind and associated cold front, apparently as a result of nearly saturated conditions in the surface-to-700-hPa layer (not shown). Further discussion of this topic is provided in section 5.

The factors associated with two of the remaining unsuccessful forecasts (cases 1 and 12) were not readily apparent and await further investigation.

4. Case applications of the downwind vector technique

a. Comparison application of the original and downwind techniques: 16 August 1997

Figure 7a shows a proximity thermodynamic sounding and wind profile associated with the incipient stage of a forward-propagating MCS that subsequently moved across northern Ohio and Pennsylvania on 16 August 1997 (case 48 in Table 1). The system developed in an environment of moderate, unidirectional westerly flow in the warm sector of a surface wave crossing southern Quebec, Canada (Fig. 7b). Large-scale forcing was weak, similar to situations described by Coniglio and Stensrud (2001) and Evans and Doswell (2001). Considerable surface-based instability was present, however, throughout the warm sector, within which afternoon temperatures warmed to above 90°F (30°C; not shown).

Using a mean wind vector of 260°/35 kt (18 m s^{-1}) and a low-level ''jet'' of 250°/32 kt (16 m s^{-1}), application of the original vector technique yields a system movement toward the east-southeast at approximately

TABLE 1. Forward-propagating MCS events used to test the downwind vector technique. Data include date/time (year + 1900, month, day, UTC hour), three-letter identification of sounding (raob) site used to calculate pertinent wind vectors, forecast (FCST) and observed (OBSVD) MCS motion [direction (DIR)/speed (SPD); speed is in knots; 1 kt is about 0.5 m s^{-1}], and direction/speed errors. Direction and speed errors exceeding 20° and 10 kt (5.0 m s^{-1}), respectively, are in boldface. The apparent source of failure for those events exceeding the above criteria is indicated in right-most column (Boundary means external boundary was present; SPRCL/RIJ means system contained supercells and/or a rear-inflow jet; Translational means system was strongly affected by the translational motion of a mesoalpha-scale environment conducive to storm initiation; Unknown means the source of error was not readily apparent). See text for details.

Case no.	Date/time (YYMMDDHH)	Raob site	Forecast motion (DIR/SPD)	Observed motion (DIR/SPD)	Direction error (FCST−OBSVD)	Speed error (FCST−OBSVD)	Apparent failure mode
1	83052000	VCT	235/60	260/55	−**25**	5	Unknown
2	83052000	DRT	245/45	265/40	−20	5	
3	83070112	PIA	270/43	290/45	−20	−2	
4	83071912	BIS	290/57	300/50	−10	7	
5	83072000	GRB	300/54	310/50	−10	4	
6	83072200	WAL	315/53	315/45	0	8	
7	87061912	AMA	295/30	315/30	−20	0	
8	87070412	UMN	280/30	290/30	−10	0	
9	87070512	UMN	270/32	270/35	0	−3	
10	87071112	STC	225/48	230/44	−5	4	
11	87072012	STC	225/41	290/35	−**65**	6	Boundary
12	87081912	OMA	290/55	320/30	−**30**	**25**	Unknown
13	87082000	UMN	310/40	330/30	−20	10	
14	87111600	LCH	260/07	260/10	0	−3	
15	88040600	SLO	255/49	270/40	−15	9	
16	88051000	HTS	280/72	270/30	10	**42**	Translational
17	88071700	ACY	325/24	315/22	10	2	
18	88081600	WAL	310/25	300/30	10	−5	
19	88081800	ACY	330/57	330/55	0	2	
20	89022112	CHS	230/51	230/37	0	**14**	Translational
21	89050500	SEP	290/53	310/65	−20	−**12**	SPRCL/RIJ
22	89050600	CHS	240/45	230/45	10	0	
23	89061700	WAL	215/46	220/45	−5	1	
24	89070212	OKC	340/50	340/50	0	0	
25	89071712	OKC	300/32	315/35	−15	−3	
26	89080600	HTS	270/30	290/25	−20	5	
27	89080700	AMA	330/25	350/25	−20	0	
28	89112100	IAD	285/60	285/55	0	5	
29	90021012	AHN	240/57	270/50	−**30**	7	Translational
30	90052800	SIL	250/30	270/30	−20	0	
31	90062000	TOP	290/40	270/45	20	−5	
32	90082612	GRB	260/27	300/30	−**40**	−3	Boundary
33	91040912	LIT	240/47	240/40	0	7	
34	91050500	GGG	240/38	250/30	−10	8	
35	91050600	AYS	270/35	270/40	0	−5	
36	91050700	ACY	240/31	270/40	−**30**	−9	Boundary
37	91052900	FNT	290/37	300/35	−10	2	
38	91070800	FNT	260/50	270/45	−10	5	
39	92070300	FNT	300/48	290/40	10	8	
40	92070300	UMN	250/47	270/45	−20	2	
41	93060412	PAH	270/50	280/52	−10	−2	
42	93060500	HAT	285/67	300/60	−15	7	
43	93080100	PAH	330/38	320/40	10	−2	
44	93080100	TOP	315/35	320/35	−5	0	
45	94041800	PIA	300/55	280/55	20	0	
46	96050512	LZK	270/40	270/70	0	−**30**	SPRCL/RIJ
47	96052112	CHH	270/50	270/60	0	−10	
48	97081612	DTX	265/40	275/45	−10	−5	

5 kt (2 m s^{-1}). As Fig. 7c (top) shows, the original vector approach depicts a scenario in which cell advection is offset almost totally by cell propagation.

However, as might be expected given the availability of dry air at midlevels (Fig. 7a), the MCS began to produce strong convective downdrafts early in its life cycle; by 1400 UTC, a well-defined cold pool was present beneath it (not shown).[4] Because the associated downdrafts brought strong westerly winds to the sur-

[4] Note that the sounding in Fig. 7a was taken around local sunrise; insolation after this time resulted in substantial boundary layer warming downwind from the incipient convective system, enhancing both updraft strength and downdraft production.

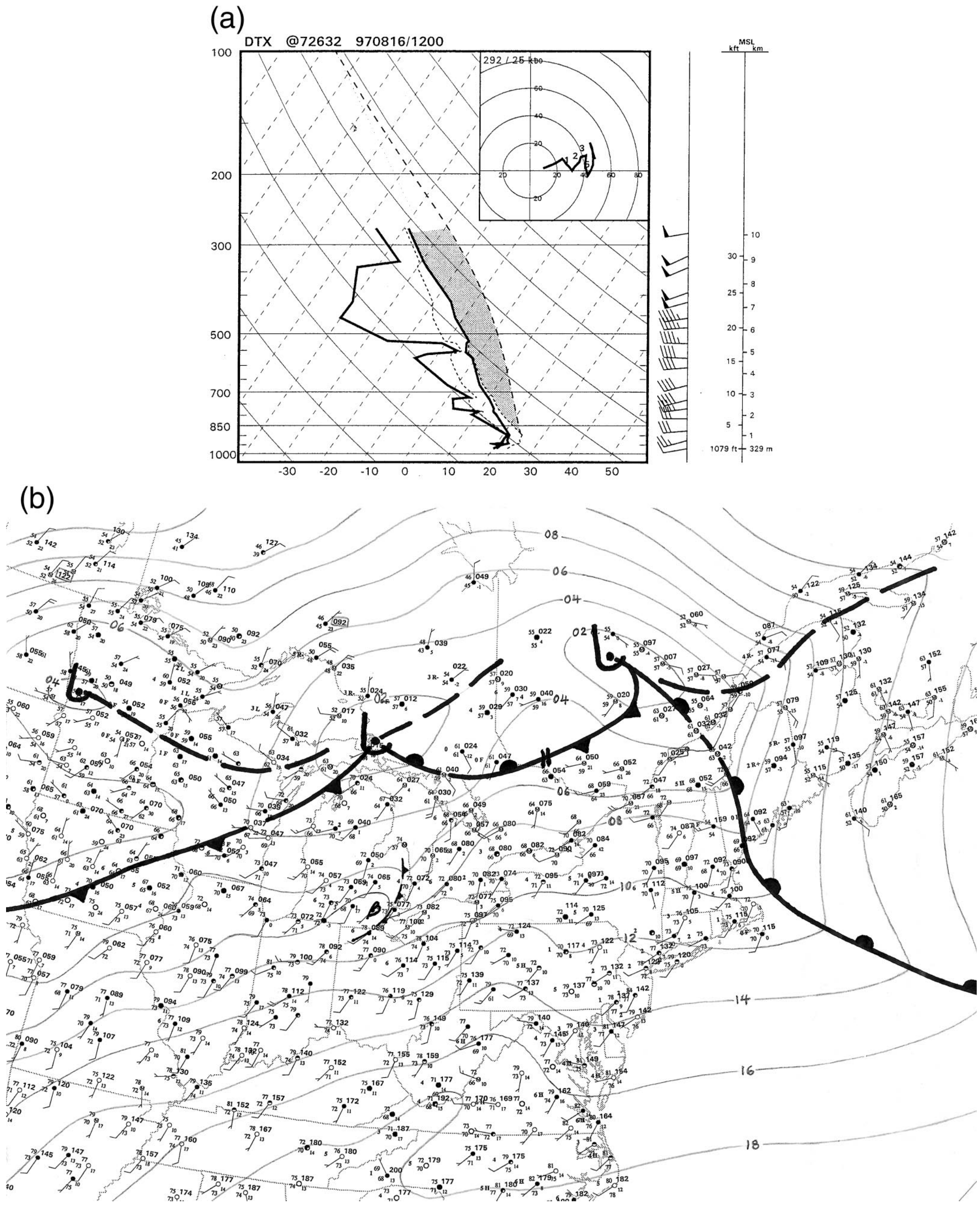

FIG. 7. (a) Same as Fig. 5a, but for White Lake, MI (near Detroit), 1200 UTC 16 Aug 1997. (b) Regional surface mesoanalysis, valid for the same time as in (a): thermodynamic data (°F), wind (kt), and pressure (hPa, with first two digits omitted); synoptic-scale boundaries are depicted with large pips, mesoalpha-scale gust front is shown with small pips, and center of the MCS mesohigh is indicated by the ‘‘B’’ (‘‘bubble high’’) over southeast Michigan. (c) (top) Application of original and (bottom) downwind versions of the vector technique to the 16 Aug 1997 MCS, based on sounding data in (a). Forecast motions are depicted by heavy solid arrows, with the MCS centroid depicted by the cross symbol. Directions are in degrees azimuth, and speeds are in knots. (d) Three-hourly radar-observed positions of leading convective line (solid lines) and severe-weather reports (damaging winds are crosses, hail is dots, and tornadoes are small squares) associated with the forward-propagating MCS of 16 Aug 1997.

face, the cold pool elongated toward the east. At the same time, capping prohibited the development of new convection toward the west (i.e., in the upwind direction), despite the fact that the near-surface flow was from the west. As a consequence, with strong system-relative convergence and instability both present in the downwind (east) direction, ascent along the progressive part of the gust front readily led to new cell development in the downwind direction, and the system propagated to the east. Because cell advection was also toward the

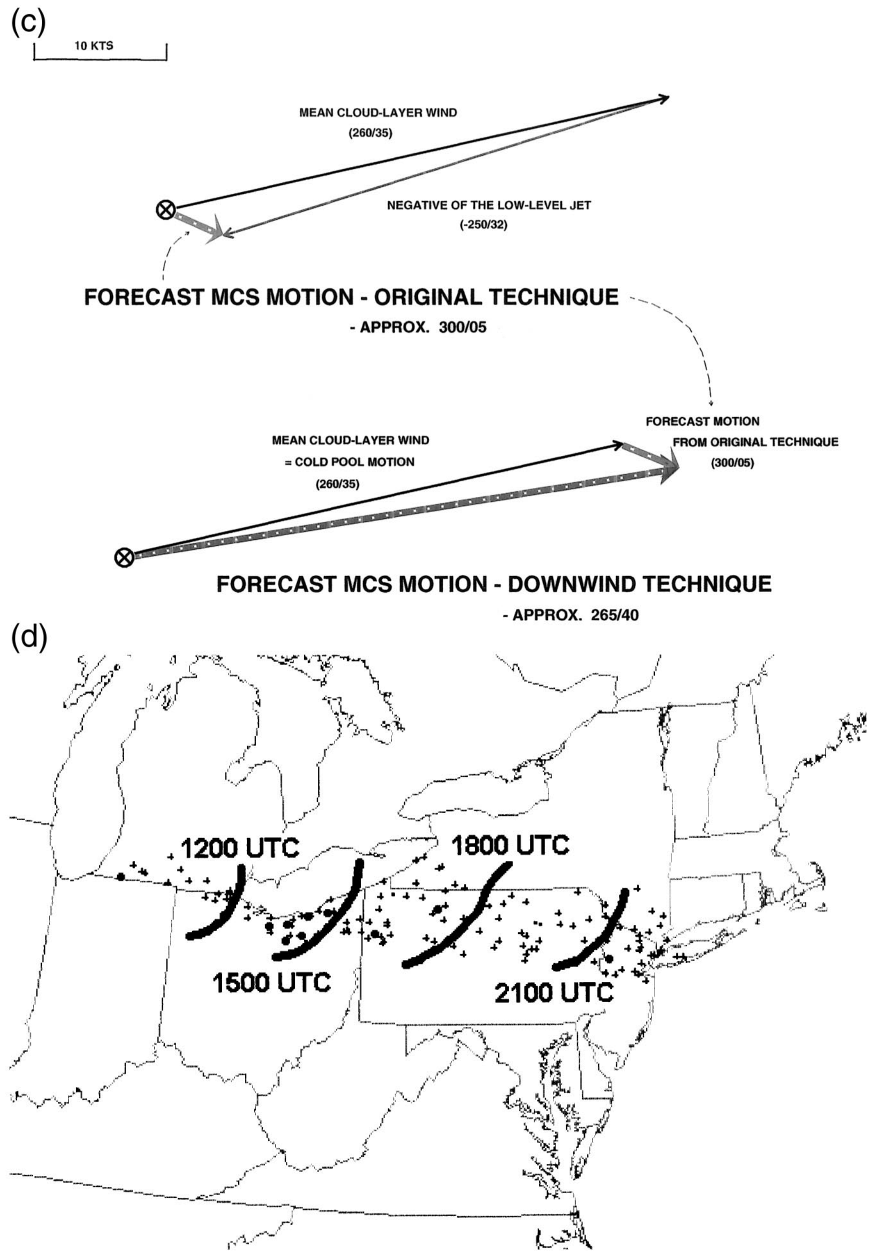

FIG. 7. (*Continued*)

east, however, advection and propagation were nearly directly additive (Fig. 7c, bottom). Thus, the MCS did not remain nearly stationary as the original vector technique would suggest but rather accelerated eastward as a forward-propagating squall line that moved at a speed faster than that of the mean wind (Fig. 7d). The downwind vector technique's motion estimate of 265° at 40 kt (20 m s^{-1}; Fig. 7c, bottom) compares favorably to the 9-h observed mean motion of 275° at 45 kt (22 m s^{-1}).

The original vector technique seriously underestimated the motion of the squall line because it failed to account for the fact that propagation would occur downwind rather than upwind. This case demonstrates the need to identify the region of greatest system-relative convergence and the distribution of surface-based conditional instability along the gust front when determining the preferred direction of propagation. Use of the 850-hPa wind or some other estimate of the low-level flow to represent propagation will yield erroneous results when convergence is maximized in a direction away from the low-level jet in the presence of conditional instability.

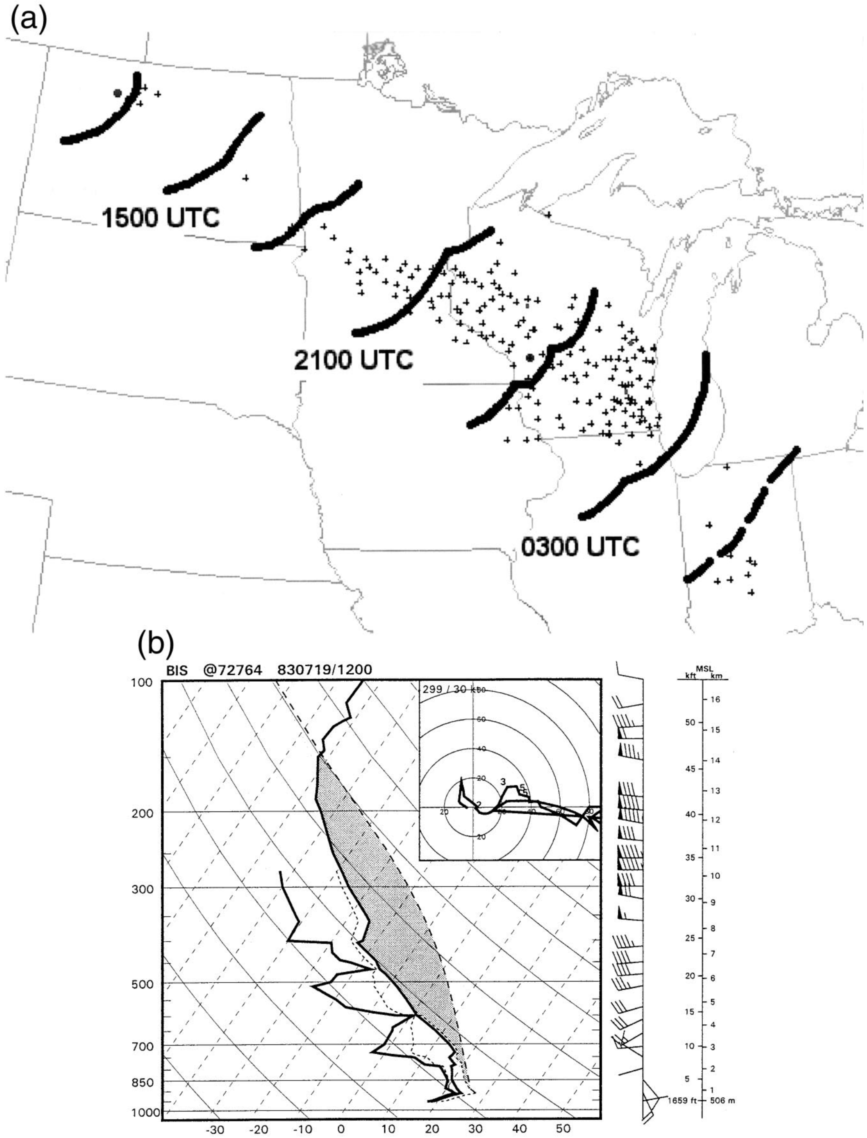

FIG. 8. (a) Same as Fig. 7d, but for the forward-propagating MCS of 19–20 Jul 1983. (b) Same as Fig. 5a, but for Bismarck, ND, 1200 UTC 19 Jul 1983. (c) Same as Fig. 7b, except valid for the same time as in (b). The center of the MCS mesohigh is indicated by the ''B'' (bubble high) over northwest North Dakota. (d) Application of the downwind vector technique for the the 19 Jul 1983 MCS, based on sounding data in (b). Directions are in degrees azimuth, and speeds are in knots. The MCS centroid is depicted by the cross symbol.

b. Application of downwind technique to a derecho: 19–20 July 1983

In the middle (low) latitudes, where the mean tropospheric flow is typically westerly (easterly), gust-front-relative flow will be enhanced when the boundary layer winds have an easterly (westerly) component. In some instances, the magnitude of gust-front-relative flow sometimes *exceeds* that of the mean cloud-layer wind. Depending upon thermodynamic conditions, convective systems developing in this kind of environment occasionally attain speeds that are more than 2 times that of the mean wind. The classic derecho of 19 July 1983, which produced a swath of widespread wind damage across the upper Mississippi Valley (Fig. 8a; see Johns and Hirt 1985), serves as an example of this type of an event.

Figure 8b, the thermodynamic sounding and wind profile taken at Bismarck, North Dakota, at 1200 UTC 19 July, is representative of conditions during the initiation of the MCS. CAPE, calculated by lifting a parcel from near 850 hPa, is substantial (around 4000 J kg^{-1}), and nearly dry adiabatic lapse rates are present at midlevels to foster strong convective downdraft development. As Fig. 8c shows, the system formed in a region

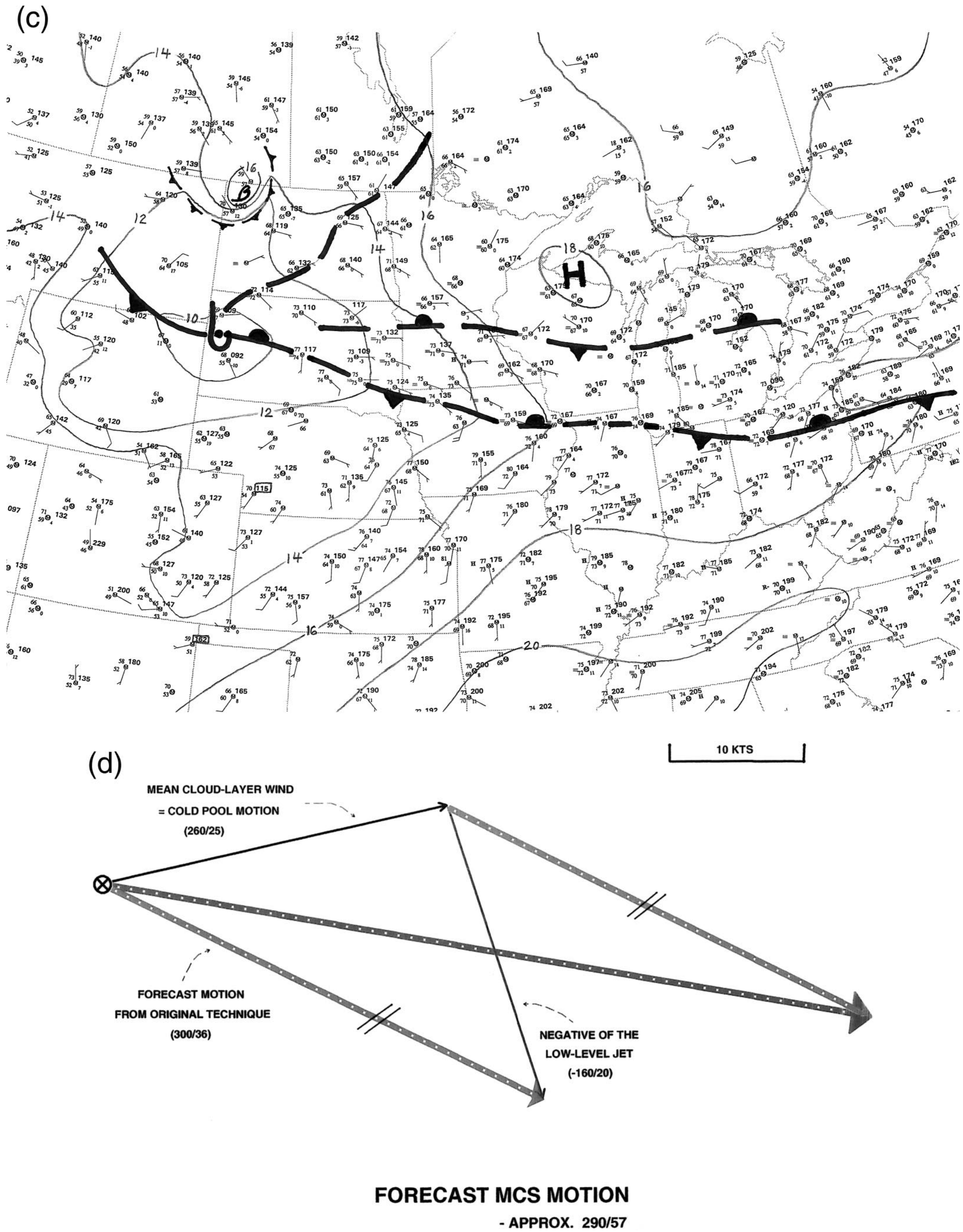

FIG. 8. (*Continued*)

of high boundary layer moisture content [average surface dewpoints around 65°F (18°C)] on the north side of a weak west–east front that had become stationary, parallel to the mid- and upper-tropospheric flow. The MCS raced east-southeast during the following 15 h, averaging more than 50 kt (25 m s^{-1}), despite the fact that the mean cloud-layer wind over the region during the period was westerly at only 25 kt (12 m s^{-1}).

Conditions were favorable for downwind development as the boundary layer moisture axis extended east into Wisconsin, and an easterly component was present in the lower levels to enhance inflow to the gust front. At the same time, capping associated with amplification of the large-scale ridge upstream from the system (not shown) prohibited convective initiation on the upwind side of the cold pool produced by the first storms over northwest North Dakota. Application of the downwind vector technique (Fig. 8d) readily illustrates how extreme system motions can be attained when cell advection and propagation are not only additive, but propagation speed is enhanced by an ''opposing'' (in this case, easterly) component to the boundary layer wind.

Another factor that can contribute to the rapid downwind movement and may have been a factor in this case is of thermodynamic origin. It is frequently noted (e.g., Johns 1993) that boundary layer moisture tends to ''pool'' on the poleward side of weak warm-season fronts, such as the one over South Dakota and Iowa (Fig. 8c). Indeed, evapotranspiration can significantly augment the local boundary layer moisture content, especially when the mixed-layer depth remains constant as a result of cloudiness and/or the presence of a frontal inversion. The added moisture lowers the level of free convection and assists convective initiation along the gust front, thereby hastening downwind propagation.

c. Application of downwind technique to a cool-season derecho: 20–21 November 1989

Although storm-scale downdrafts are believed to originate primarily above the lifting condensation level (Wakimoto 2001), some of the cases examined in this study suggest that forward propagation may also be fostered by mesohigh development associated with the presence of dry air in the *subcloud* layer. This ''organized microburst'' MCS mode occurs most frequently in arid regions, although systems of this kind occasionally develop elsewhere when moisture is sparse but steep lower-tropospheric lapse rates are present to enhance convective downdraft development. For example, several mesosystems of this type have produced significant wind damage in the mid-Atlantic region and over the Midwest and plains in recent years. Moisture in such situations is often so limited that thunderstorms can only develop where sustained convergence is provided by a gust front, orography, or some other mechanical initiating mechanism. Once storms do form, the resulting MCS is sustained by a downwind succession of microbursts.

Operational experience has shown that systems that form in environments of this kind typically display weak radar reflectivities but can produce devastating winds. For example, in the 20 November 1989 case discussed here, thunderstorm echo tops associated with the evening squall line were at or below 20 000 ft (7 km), and maximum reflectivities were less than 30 dB*Z*. Nevertheless, the storms produced a continuous swath of damaging winds from central Pennsylvania into southeast New York and southern New England, with measured gusts in excess of 70 kt (35 m s^{-1}; Fig. 9a).

The environment across the mid-Atlantic region on the afternoon of 20 November was characterized by fast, largely unidirectional west-northwesterly flow in advance of a short-wave disturbance and cold front over the upper Great Lakes (not shown). Modified, dry polar air was present ahead of the front. Because boundary layer moisture was limited [surface dewpoints below 45°F (7°C)], CAPE was minimal (Figs. 9b,c; note that, because the sounding site was south of the MCS track and south of the associated midlevel jet streak, an inversion is depicted at 700 hPa that was substantially weaker or nonexistent farther north). Nevertheless, lapse rates were steep, especially for the time of the year and the region. Sunshine and westerly (downslope) flow east of the Appalachians warmed afternoon surface temperatures to the mid-60s Fahrenheit (18–20°C) over the lower elevations of eastern Pennsylvania and New Jersey, producing large dewpoint depressions.[5] The warm air enhanced the buoyancy, fostering late-day thunderstorm development along the cold front in central Pennsylvania. Sustained uplift along the front and ideal conditions for cold downdraft production allowed the storms to grow quickly into a linear MCS. Because storm advection and propagation were additive, the system accelerated southeastward at nearly 60 kt (30 m s^{-1}), more than 20 kt (10 m s^{-1}) faster than the mean cloud-layer wind (Fig. 9d).

5. Practical aspects of application

a. Elevated systems

A significant forecast problem involving MCS development on the cool side of surface boundaries is determining whether the system will remain elevated or will at some point become ''rooted'' in the boundary layer. Dependent as they are on the existence of surface-based convection along a gust front, it is clear that neither the original nor downwind versions of the vector scheme can be applied to a purely elevated MCS. Determining the potential for surface-based development with an elevated MCS is difficult, although systems with strong cold pools and relatively warm/moist ''cool'' sectors are good candidates. In the 19–20 July 1983 event, for example, daytime heating eroded the shallow skin layer present in the morning over North Dakota (Fig. 8b), resulting in a deep afternoon mixed layer over Minnesota and Wisconsin (not shown). This allowed boundary layer parcels north of the stationary front to be lifted along the gust front, contributing to the rapid downstream propagation observed. It should not be assumed, however, that an MCS will remain completely elevated just because the low-level air is cold (e.g., Schmidt and Cotton 1989). Upon selection of a representative ''inflow'' wind, the vector technique may, of course, always be used to estimate future system motion if it appears that an elevated MCS might become surface based.

[5] Such environments, in theory, are characterized by a substantial degree of downdraft CAPE (DCAPE). Because of the limitations of parcel theory used in its development DCAPE is often *not* a reliable estimator of cold-pool strength, especially in the presence of substantial shear (Gilmore and Wicker 1998).

b. MCSs containing supercells and mesoscale vortices

The presence of embedded supercells can significantly affect MCS evolution and motion. Many MCSs, especially those that produce derechos, initiate as supercells (e.g., Johns and Leftwich 1988; Klimowski et al. 2000). In other cases, the onset of forward propagation and bow-echo development appears to be related to the appearance of rotating updrafts in existing convection [e.g., the Texas derecho of 4 May 1989 (Smith 1990) and the 17 August 1994 Lahoma, Oklahoma, event (Janish et al. 1996)]. At the same time, embedded supercells sometimes occur in back-building or quasi-stationary convection [e.g., Texas to Mississippi, 15–16 November 1987 (Corfidi et al. 1990) and Arkansas/Tennessee, 1 March 1997 (Rogash et al. 2000)].

As Schmidt and Cotton (1989) and others have shown, the presence of a supercell can drastically alter storm-scale flow within an MCS, thereby influencing its overall motion, strength, and longevity. For example, in a case included in the developmental sample for the downwind vector technique (case 46 in Table 1; Spoden et al. 1998), forecast speed was significantly underestimated [forecast: 40 kt (20 m s^{-1}); observed: 70 kt (35 m s^{-1})], although the system's eastward motion was correctly depicted. The presence of a strong, cyclonic circulation in the northern part of the MCS may have hastened the system's forward movement by increasing westerly flow in the cold pool. In a case presented by Schmidt and Cotton (1989), redistribution of the precipitation cascade by a persistent rotating storm in an elevated squall line altered the shape of the system's cold pool. This not only affected storm propagation, but also the location of strongest surface winds. It is also worth noting that the presence of ''book-end vortices'' can hasten MCS motion by fostering the development of rear-inflow jets (e.g., Weisman 1993).

Long-lasting MCSs sometimes contain larger-scale convectively induced circulations known as mesoscale vorticity centers (MCVs). These features, which develop in response to Coriolis acceleration of the rear-to-front or front-to-rear flow and/or in response to tilting and stretching of environmental and system-generated vorticity, also affect MCS motion and longevity (e.g., Brandes 1990; Bartels and Maddox 1991; Davis and Weisman 1994; Skamarock et al. 1994; Trier et al. 1997; Weisman and Davis 1998). The original dataset of Corfidi et al. (1996) and the cases examined for the downwind vector technique include events with both MCVs and supercells. In fact, the prominent mesoscale vortex associated with one of the cases in the original study (6–7 July 1982) was the subject of detailed investigation (Menard and Fritsch 1989). Absence of high-resolution radar data precludes an accurate assessment of the relative frequency of MCVs and supercells in the datasets used to develop the vector technique. It is clear that the influence of supercells and other vortices is too complex to be addressed explicitly by the scheme. Nevertheless, because the collective impact of these features was an unwitting factor in its development, the presence of a supercell or MCV in a given MCS does *not* necessarily mean that the technique will yield erroneous results.

c. Influence of the background synoptic-scale environment

The advective component of MCS motion becomes increasingly dominant relative to propagation as the translational motion of the background synoptic-scale ''support'' for an MCS increases. This effect is most apparent in conjunction with cool-season serial bow MCSs (Johns and Hirt 1987). Because the support (usually a short-wave trough) in such cases often moves rapidly, and because nearly saturated conditions and/or inversions are typically present in the lower troposphere to limit downwind propagation, the vector technique often overestimates the motion of serial bows, as was noted in section 3. With the convection confined to a narrow zone of forced ascent along a front, systems of this kind essentially move with the speed of the associated synoptic-scale disturbance.

Although it is often not obvious to the casual observer, the translational speed of an MCS's synoptic support can significantly influence the sensible weather produced by the system. For example, cold fronts in environments of strong, largely unidirectional flow are often accompanied by quasi-linear MCSs (Hobbs and Persson 1982). These systems sometimes exhibit considerable forward motion because of movement of the front (and the short-wave trough) and therefore often do not yield excessive rainfall. Inspection of time-lapse radar data and application of the original vector technique reveals, however, that many such MCSs are actually quasi stationary or back building relative to the front. The absence of excessive precipitation reflects the ''external'' component of motion that maintains system progression.

An example of this kind of event occurred in conjunction with an intense cyclone over the Mississippi Valley on 9–10 November 1998. The linear MCS in question extended for more than 400 n mi (740 km), embedded in deep unidirectional southwest flow ahead of a progressive short-wave trough (Fig. 10a). The narrow line of forced convection moved northeast at 30 kt (15 m s^{-1}), roughly with the speed of the cold front/upper trough responsible for its development. The thermodynamic environment (not shown) was such that surface-based storm initiation was prohibited except along the front, and cold convective downdraft potential was minimal. As a result, the weak cold pool that did develop elongated parallel to the mean flow, and individual storms trained from south to north along the boundary as the convective system swept northeastward. Rain was briefly heavy as the line passed, but excessive rainfall

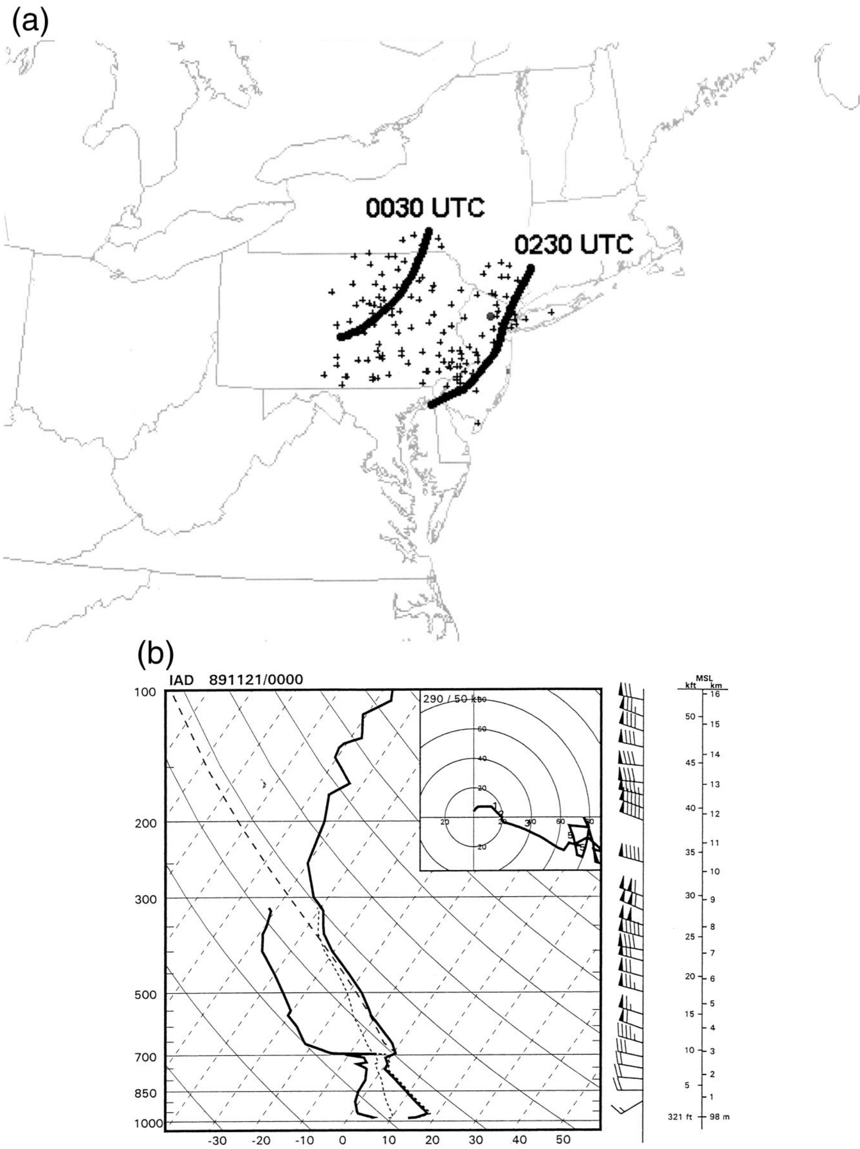

FIG. 9. (a) Same as Fig. 7d, but for the forward-propagating MCS of 20–21 Nov 1989. (b) Same as Fig. 5a, but for Sterling, VA (near Washington, DC), 0000 UTC 21 Nov 1989. (c) Same as Fig. 7b, except valid 1800 UTC 20 Nov 1989. (d) Same as Fig. 8d, but for the 20–21 Nov 1989 MCS and based on sounding data in (c).

did not occur because of the external motion provided by the synoptic-scale trough.

In contrast, extensive flooding accompanied a similar convective system that moved very slowly across southern California on 6 February 1998. The California MCS, like the one over the central United States, was also embedded in large-scale southwest flow ahead of a deep trough. The translational motion of the region conducive to thunderstorm development was limited in the California event, however, because the large-scale pattern was much less progressive (Fig. 10b). The short-wave impulse approaching southern California at 1200 UTC 6 February lifted north-northeast to off of the Oregon coast on 7 February, maintaining deep, unidirectional southwesterly flow over the affected region for an extended period. As a result, excessive rainfall did occur, and the training/back-building nature of the embedded convection was more readily apparent than in the November event.

d. Environments of weak mean flow

In contrast to the systems embedded in strong mean flow, the motion of convective systems in weak flow is dominated by propagation. The advective component

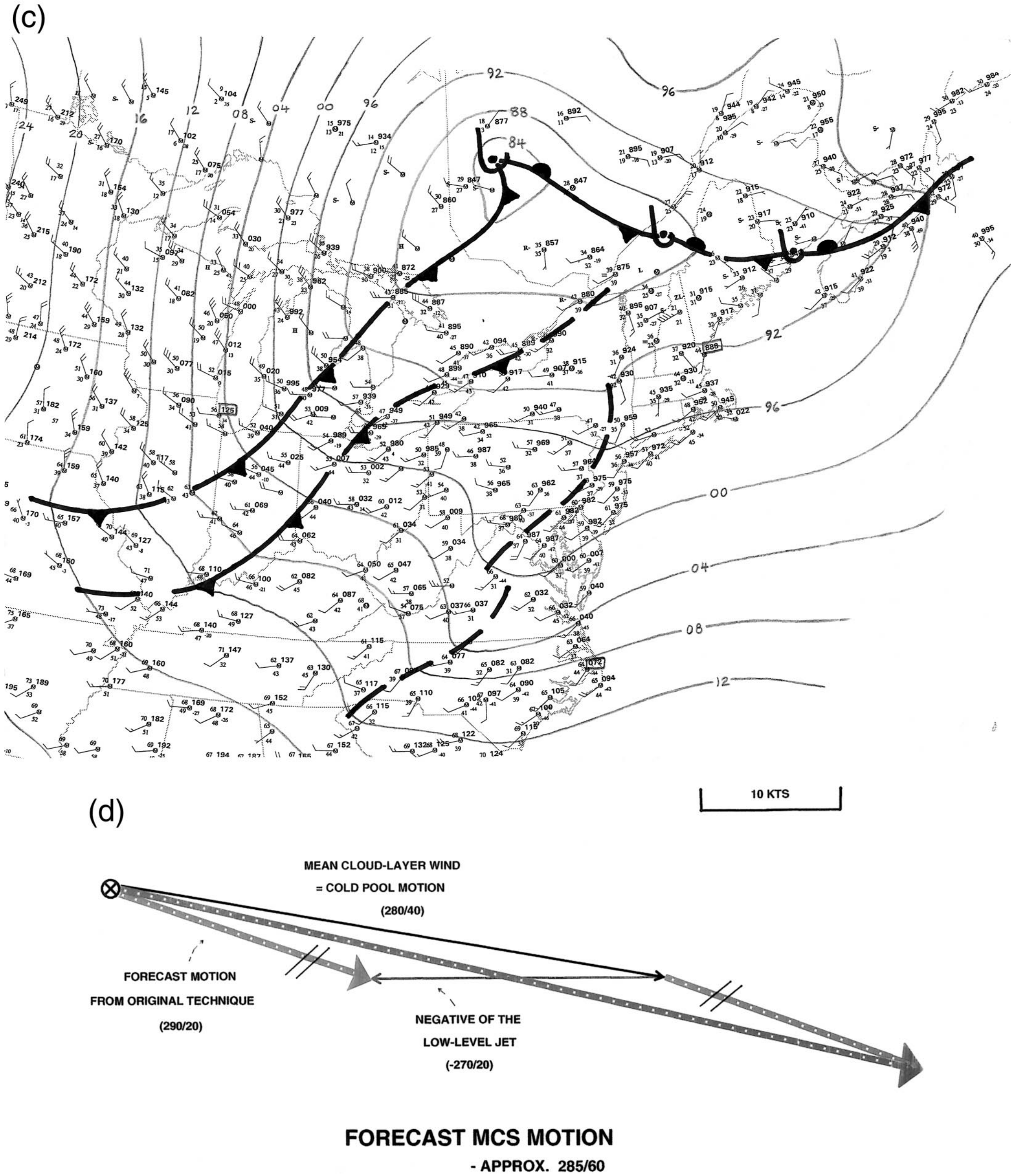

FIG. 9. (*Continued*)

nevertheless remains important in determining the most favored *direction* for propagation.

The combination of strong propagation and weak advection accounts for the somewhat unusual behavior of the convective clusters that occasionally produce damaging winds in the Phoenix, Arizona, area each summer. Such systems are typically associated with modest east to northeasterly midtropospheric flow (e.g., Maddox et al. 1995; McCollum et al. 1995). Northeasterly midlevel winds and downslope flow favor the southwestward motion of gust fronts produced by diurnal thunderstorms forming over the high terrain north and east of the city. Convergence along the convective outflow, coupled with the presence of steep lower-tropospheric lapse rates and large dewpoint depressions, fosters additional downdraft development. This outflow drives convective initiation sequentially southwest across central and southern Arizona through the day. Depending upon the boundary layer moisture availability over the lower deserts, such activity sometimes propagates as far southwest as southern California. The extent to which propagation is involved in system motion is one of the more unique characteristics of organized severe convection in Arizona, and systems of this kind are generally well forecast by the downwind vector technique.

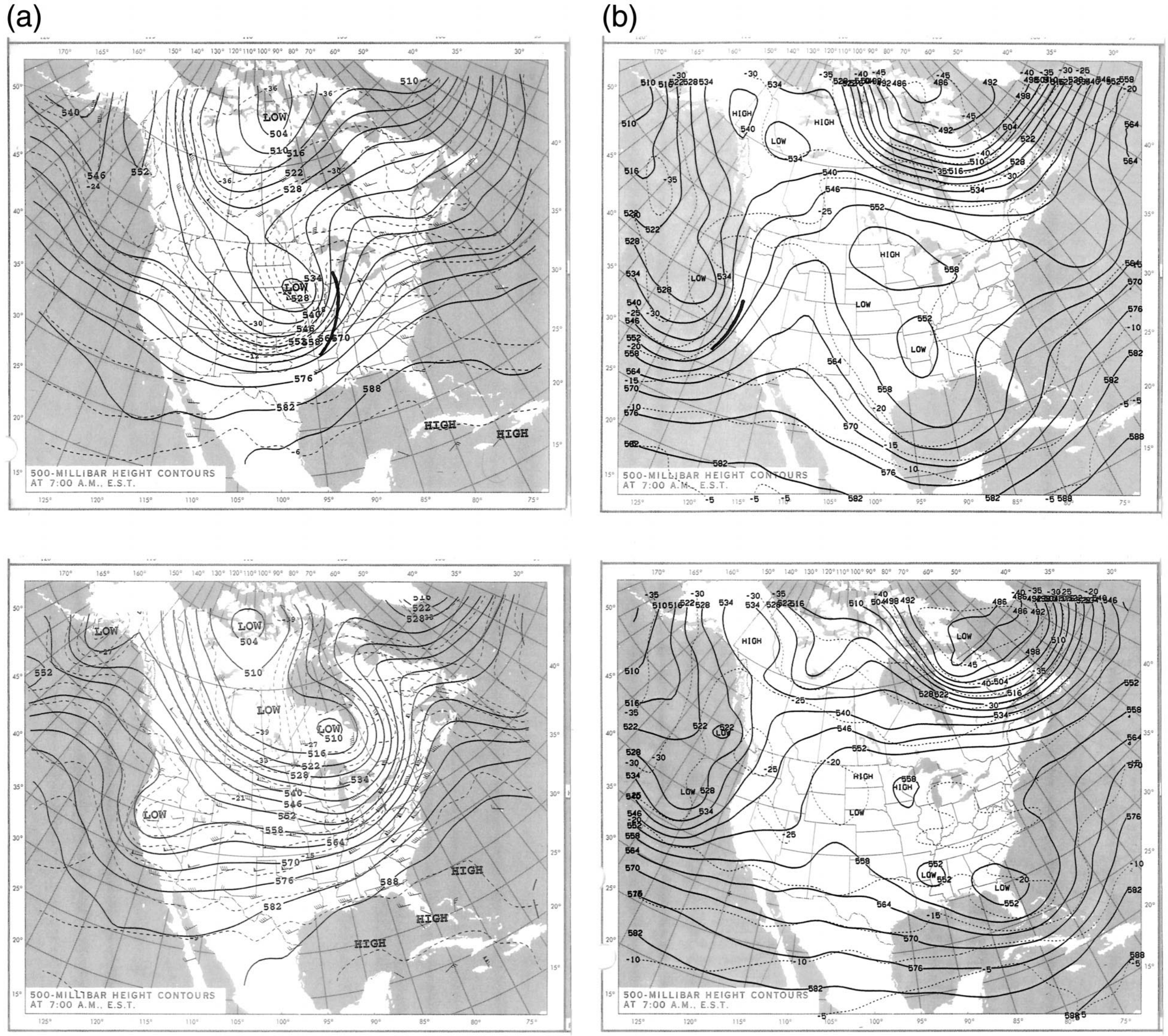

FIG. 10. (a) National Oceanic and Atmospheric Administration daily weather map of North American 500-hPa height analyses at (top) 1200 UTC 10 Nov and (bottom) 1200 UTC 11 Nov 1998. Heights (dam) are depicted by solid lines, and temperatures (°C) are shown by dashed lines. Heavy solid line denotes the position of the linear MCS at map time. (b) Same as (a), but for (top) 1200 UTC 6 Feb and (bottom) 1200 UTC 7 Feb 1998.

e. Computation of mean wind/cold-pool motion and low-level inflow

Little has been said thus far about the depth of the layer used to compute cloud-layer mean wind (in the original technique) and cold-pool motion (in the downwind version). The layer used in the developmental datasets, 850–300 hPa, was chosen because inclusion of 200-hPa data was found, on average, to overestimate observed cell speed and, hence, the cloud-layer mean winds computed for the original (Corfidi et al. 1996) study.

Examination of several recent forward-propagating systems that moved faster than forecast by the downwind technique suggests, however, that the underestimation may in fact have been due in part to exclusion of data above 300 hPa. Because each case was characterized by very large (i.e., greater than 5000 J kg^{-1}) surface-based CAPE, it is speculated that a substantial amount of cloud material was likely present above 300 hPa and/or that the cold pools were stronger and, therefore, faster moving than average. Use of wind data up to 200 hPa is encouraged when calculating the mean wind in regions of very high CAPE.

Careful consideration should also be given to the depth of the layer used to estimate the low-level jet (or, more proper, the propagation component) in the vector scheme, because propagation is so sensitive to the lower-tropospheric flow. Definitions suggested by Bonner (1968) were used to identify low-level jets in the original

(Corfidi et al. 1996) study. Given our limited understanding of the microphysical and cloud-scale aspects of thunderstorm initiation and given the constraints of parcel theory (e.g., Ziegler and Rasmussen 1998), it is clear that selection of the most appropriate inflow layer is best made on a case-by-case basis. For ease of calculation, the maximum wind in the lowest 5000 ft (1.5 km) was found to provide a useful estimate in most of the events used in the current study, but a somewhat deeper layer might prove more appropriate when the lifting condensation level is very high.

6. An MCS continuum

For the purposes of discussion, the MCSs in this presentation have been referred to as being of either the forward- or backward-propagating type. In reality, of course, the interplay of variables that affect MCS propagation is complex and may vary over space and time. As a result, observed systems typically exhibit a continuum of MCS propagational modes. Section 2 shows that a given MCS may simultaneously exhibit both upwind and downwind development. The tendency for downwind or upwind development may also change over time. Forward-propagating systems, for example, sometimes assume back-building characteristics later in their life cycles, or at least periods of diminished downwind development. This change may occur as a result of moistening of the low to midtroposphere by nearby convection (which decreases negative buoyancy) and/or as a result of diurnal cooling (which reduces potential for new cell development). An event that exhibited such evolution was the 4 October 1998 MCS in Kansas City. Because propagation in real-life systems is rarely purely of one form or another, in general, *it is advantageous to recompute or slightly modify previously calculated motion vectors to account for varying degrees of forward propagation along the gust front over space and time*. This recomputation may require multiple ‘‘local refinements’’ to previously computed vector calculations during the life of an event.

Researchers in recent decades have identified many of the synoptic and mesoalpha-scale meteorological patterns associated with MCSs that produce hazardous weather such as excessive rainfall. These valuable investigations have enhanced recognition of impending weather threats and have helped to increase warning lead times. In some instances, however, it appears that attention has been focused on enumerating minor differences that might exist between events occurring in different geographical areas or seasons at the expense of emphasizing those characteristics universal to MCS-induced weather hazards in general. For example, the Johnstown flood in July of 1977 was one of the most notorious mesohigh flash floods to have occurred in recent years. Analysis reveals, however, that the mesoalpha-scale meteorological setup of the Johnstown tragedy was very similar to that of the October 1998 flood in Kansas City, even though the synoptic environments of the two events were much different.[6] Both featured a mesoscale outflow boundary that had become parallel to the mean cloud-layer flow in a moist, largely unidirectional wind regime, and, in both cases, the boundary remained stationary for an extended period of time.

In lieu of pattern recognition, it seems advantageous to focus on the salient *processes* common to such events almost universally, regardless of the prevailing synoptic, geographical, or seasonal environment. This idea is in accord with the ingredients-based approach to forecasting advocated by Doswell et al. (1996), and the vector concept can be used to facilitate it. For example, from a vector perspective, it is apparent that back-building MCSs, lake-effect convective plumes (Peace and Sykes 1966; Niziol 1987), cool-season convective trains (Reynolds 1998), and many cold-frontal rainbands are, in fact, regional and/or seasonal variations of a common kinematic and thermodynamic theme: the presence of weak, unidirectional cloud-layer flow in a nearly saturated environment, with a slow-moving or stationary initiating mechanism. Lake-effect plumes produce heavy snow for much the same reason that back-building MCSs produce flash floods: system propagation is offset by advection, and the initiating mechanism (a lake-enhanced boundary in the case of snowbands; a gust front in the case of a back-building MCS) remains nearly stationary.

7. Summary

A more complete technique for estimating short-term MCS motion that builds on the work of Corfidi et al. (1996) has been presented. It is based on the fact that the preferred direction of system propagation (i.e., the location of new cell development relative to existing activity) is not always determined by the low-level jet. Propagation direction is, instead, more generally dictated by the location of maximum gust-front convergence in the presence of conditional instability. For some convective systems (in particular, many MCCs), the location of maximum gust-front convergence is, indeed, in the direction of the low-level jet. Because their advective motion is partially offset by propagation, MCSs of this kind tend to move more slowly than the mean cloud-layer flow. For these systems, the original vector technique may be used to provide a forecast of MCS motion.

In contrast, the greatest gust-front convergence occurs on the downwind or forward side of bow-echo and derecho-producing convective systems. Such systems develop when conditions are supportive of downstream convective development along a gust front. Because the advective and propagation components of overall system motion are additive, these MCSs sometimes move

[6] The Johnstown flood occurred near the axis of a broad upper-level anticyclone, whereas the Kansas City event occurred on the eastern side of a progressive, large-amplitude short-wave trough.

faster than the mean wind. The downwind vector scheme may be used to estimate their motion.

In part because system cold pools tend to elongate in the direction of the mean wind over time, environments of strong flow with minimal cloud-layer shear may be associated with both forward-propagating MCSs and quasi-stationary and/or back-building systems. This situation is especially true when wind profiles are unidirectional. Portions of the gust front that align parallel to the mean flow become favorable sites for upstream development, whereas parts that orient perpendicularly become supportive of downstream development. This observation, coupled with knowledge of the spatial and temporal distribution of surface-based instability, may be used to determine whether cell propagation will be directed primarily upwind or downwind and, therefore, whether a system will exhibit forward or back-building development (or perhaps both) during its evolution (appendix).

Based as it is on simple assumptions about cold-pool behavior and motion, the vector technique can, at best, provide only a rough estimate of MCS movement. The scheme could be refined by incorporating more detailed real-time thermodynamic data that describe the potential for convective downdraft development than are now available. The technique, however, may be used with both observed data and model output, and it can assist in anticipating the predominant convective mode that will be assumed by an incipient MCS. The scheme also may be used to visualize better the constant interplay between cell advection and propagation that accounts for observed MCS motion.

Acknowledgments. The author thanks P. Banacos, D. Blahyj, C. Doswell, J. Evans, S. Goss, D. Imy, R. Johns, J. Kain, C. Mead, J. Moore, J. Racy, D. Schultz, D. Stensrud, R. Thompson, and S. Weiss for valuable comments and P. Banacos, G. Carbin, and P. Janish for assistance with figures. Special thanks are given to J. Evans for providing data on forward-propagating systems. Thanks also are given to R. Grumm, R. Maddox, B. Schwartz, and an anonymous reviewer for providing substantial constructive criticism of the manuscript.

APPENDIX

Summary of Cold-Pool Factors that Affect MCS Propagation

1) A cold pool will elongate in the direction of the mean cloud-layer wind as a result of momentum transfer.
2) The degree of elongation increases as the wind profile becomes more unidirectional, and this effect occurs on all time- and space scales.
3) Propagation, or new cell development relative to existing storms, occurs most readily on the periphery of the cold pool (i.e., along those portions of the gust front), where the relative inflow is strongest and where surface-based convective instability is present:
   (a) upwind-developing MCSs are most favored along quasi-stationary (mean flow parallel) portions of the gust front, and
   (b) downwind-developing MCSs are favored on the more progressive (mean flow perpendicular) parts of the boundary.
4) Thermodynamic factors modulate the role played by gust-front orientation and motion:
   (a) upwind-developing environments are characterized by comparatively moist conditions through the low to midtroposphere and, therefore, relatively weak convective-scale downdrafts, and
   (b) downwind-developing environments are characterized by comparatively dry conditions at midlevels and/or in the subcloud layer and, therefore, a tendency to produce strong convective-scale downdrafts.

REFERENCES

Bartels, D. L., and R. A. Maddox, 1991: Midlevel cyclonic vortices generated by mesoscale convective systems. *Mon. Wea. Rev.,* **119,** 104–118.

Bluestein, H. B., and M. H. Jain, 1985: Formation of mesoscale lines of precipitation: Severe squall lines in Oklahoma during spring. *J. Atmos. Sci.,* **42,** 1711–1732.

Bonner, W. J., 1968: Climatology of the low-level jet. *Mon. Wea. Rev.,* **96,** 833–850.

Bosart, L. F., and F. Sanders, 1981: The Johnstown Flood of July 1977: A long-lived convective system. *J. Atmos. Sci.,* **38,** 1616–1642.

Brandes, E. A., 1990: Evolution and structure of the 6–7 May 1985 mesoscale convective system and associated vortex. *Mon. Wea. Rev.,* **118,** 109–127.

Chappell, C. F., 1986: Quasi-stationary convective events. *Mesoscale Meteorology and Forecasting,* P. S. Ray, Ed., Amer. Meteor. Soc., 289–310.

Charba, J. P., 1974: Application of gravity current model to analysis of squall-line gust front. *Mon. Wea. Rev.,* **102,** 140–156.

Coniglio, M. C., and D. J. Stensrud, 2001: Simulation of a progressive derecho using composite initial conditions. *Mon. Wea. Rev.,* **129,** 1593–1616.

Corfidi, S. F., 1998: Forecasting MCS mode and motion. Preprints, *19th Conf. on Severe Local Storms,* Minneapolis, MN, Amer. Meteor. Soc., 626–629.

——, N. W. Junker, and F. H. Glass, 1990: The Louisiana/Mississippi flash flood and severe outbreak of 15–16 November 1987. Preprints, *16th Conf. on Severe Local Storms,* Kananaskis Park, AB, Canada, Amer. Meteor. Soc., 627–633.

——, J. H. Merritt, and J. M. Fritsch, 1996: Predicting the movement of mesoscale convective complexes. *Wea. Forecasting,* **11,** 41–46.

Davis, C. A., and M. L. Weisman, 1994: Balanced dynamics of mesoscale vortices produced in simulated convective systems. *J. Atmos. Sci.,* **51,** 2005–2030.

Doswell, C. A., III, H. E. Brooks, and R. A. Maddox, 1996: Flash flood forecasting: An ingredients-based methodology. *Wea. Forecasting,* **11,** 560–581.

Droegemeier, K. K., and R. B. Wilhelmson, 1987: Numerical simulation of thunderstorm outflow dynamics. Part 1: Outflow sensitivity experiments and turbulence dynamics. *J. Atmos. Sci.,* **44,** 1180–1210.

Evans, J. S., and C. A. Doswell III, 2001: Examination of derecho environments using proximity soundings. *Wea. Forecasting,* **16,** 329–342.

Fovell, R. G., and Y. Ogura, 1989: Effect of vertical wind shear on

numerically simulated multicell storm structure. *J. Atmos. Sci.,* **46,** 3144–3176.
Gilmore, M. S., and L. J. Wicker, 1998: The influence of midtropospheric dryness on supercell morphology and evolution. *Mon. Wea. Rev.,* **126,** 943–958.
Goff, R. C., 1976: Vertical structure of thunderstorm outflows. *Mon. Wea. Rev.,* **104,** 1429–1440.
Hamilton, R. E., 1970: Use of detailed intensity radar data in mesoscale surface analysis of the July 4, 1969 storm in Ohio. Preprints, *14th Radar Meteorology Conference,* Tucson, AZ, Amer. Meteor. Soc., 339–342.
Hobbs, P. V., and O. G. Persson, 1982: The mesoscale and microscale structure and organization of clouds and precipitation in midlatitude cyclones. Part V: The substructure of narrow cold-frontal rainbands. *J. Atmos. Sci.,* **39,** 280–295.
Houze, R. A., Jr., 1993: *Cloud Dynamics.* Academic Press, 570 pp.
Hoxit, L. R., R. A. Maddox, C. F. Chappell, F. L. Zuckerberg, H. M. Mogil, and I. Jones, 1978: Meteorological analysis of the Johnstown, PA flash flood, 19–20 July 1977. NOAA Tech. Rep. ERL 401-APCL 43, 71 pp.
Janish, P. R., R. H. Johns, and K. C. Crawford, 1996: An evaluation of the 17 August 1994 Lahoma, Oklahoma, supercell/MCS event using conventional and non-conventional analysis and forecasting techniques. Preprints, *18th Conf. on Severe Local Storms,* San Francisco, CA, Amer. Meteor. Soc., 76–80.
Johns, R. H., 1993: Meteorological conditions associated with bow echo development in convective storms. *Wea. Forecasting,* **8,** 294–299.
——, and W. D. Hirt, 1985: The derecho of July 19–20, 1983 . . . A case study. *Natl. Wea. Digest,* **10,** 17–32.
——, and ——, 1987: Derechos: Widespread convectively induced windstorms. *Wea. Forecasting,* **2,** 32–49.
——, and P. W. Leftwich, 1988: The severe thunderstorm outbreak of 28–29 July 1986: A case exhibiting both isolated supercells and a derecho-producing convective system. Preprints, *15th Conf. on Severe Local Storms,* Baltimore, MD, Amer. Meteor. Soc., 448–451.
——, K. W. Howard, and R. A. Maddox, 1990: Conditions associated with long-lived derechos: An examination of the large-scale environment. Preprints, *16th Conf. on Severe Local Storms,* Kananaskis Park, AB, Canada, Amer. Meteor. Soc., 408–412.
Junker, N. W., R. S. Schneider, and S. L. Fauver, 1999: A study of heavy rainfall events during the Great Midwest Flood of 1993. *Wea. Forecasting,* **14,** 701–712.
Klimowski, B. A., R. Przybylinski, G. Schmocker, and M. R. Hjelmfelt, 2000: Observations of the formation and early evolution of bow echoes. Preprints, *20th Conf. on Severe Local Storms,* Orlando, FL, Amer. Meteor. Soc., 44–47.
Maddox, R. A., 1980: Mesoscale convective complexes. *Bull. Amer. Meteor. Soc.,* **61,** 1374–1387.
——, C. F. Chappell, and L. R. Hoxit, 1979: Synoptic and meso-α scale aspects of flash flood events. *Bull. Amer. Meteor. Soc.,* **60,** 115–123.
——, D. M. McCollum, and K. W. Howard, 1995: Large-scale patterns associated with severe summertime thunderstorms over central Arizona. *Wea. Forecasting,* **10,** 763–778.
McCollum, D. M., R. A. Maddox, and K. W. Howard, 1995: Case study of a severe mesoscale convective system in central Arizona. *Wea. Forecasting,* **10,** 643–665.
Menard, R. D., and J. M. Fritsch, 1989: A mesoscale convective complex–generated inertially stable warm core vortex. *Mon. Wea. Rev.,* **117,** 1237–1261.
Merritt, J. H., and J. M. Fritsch, 1984: On the movement of the heavy precipitation areas of mid-latitude mesoscale convective complexes. Preprints, *10th Conf. on Weather Analysis and Forecasting,* Clearwater Beach, FL, Amer. Meteor. Soc., 529–536.
Moore, J. T., C. H. Pappas, and F. H. Glass, 1993: Propagation characteristics of mesoscale convective systems. Preprints, *17th Conf. on Severe Local Storms,* St. Louis, MO, Amer. Meteor. Soc., 538–541.
Newton, C. W., and S. Katz, 1958: Movement of large convective rainstorms in relation to winds aloft. *Bull. Amer. Meteor. Soc.,* **39,** 129–136.
Niziol, T. A., 1987: Operational forecasting of lake effect snowfall in western and central New York. *Wea. Forecasting,* **2,** 310–321.
Orlanski, I., 1975: A rational subdivision of scales for atmospheric processes. *Bull. Amer. Meteor. Soc.,* **56,** 527–530.
Parker, M. D., and R. H. Johnson, 2000: Organizational modes of midlatitude mesoscale convective systems. *Mon. Wea. Rev.,* **128,** 3413–3436.
Peace, R. L., and R. B. Sykes Jr., 1966: Mesoscale study of a lake effect snowstorm. *Mon. Wea. Rev.,* **94,** 495–507.
Pontrelli, M. D., G. Bryan, and M. Fritsch, 1999: The Madison County, Virginia, flash flood of 27 June 1995. *Wea. Forecasting,* **14,** 384–404.
Przybylinski, R. W., 1995: The bow echo: Observations, numerical simulations, and severe weather detection methods. *Wea. Forecasting,* **10,** 203–218.
Purdom, F. W., 1973: Meso-highs and satellite imagery. *Mon. Wea. Rev.,* **101,** 180–181.
Ray, P., 1990: Convective dynamics. *Radar in Meteorology,* D. Atlas, Ed., Amer. Meteor. Soc., 348–400.
Reynolds, D. W., 1998: Cool season convective trains. Preprints, *16th Conf. on Weather Analysis and Forecasting,* Phoenix, AZ, Amer. Meteor. Soc., 199–201.
Rogash, J. A., and R. D. Smith, 2000: Multiscale overview of a violent tornado outbreak with attendant flash flooding. *Wea. Forecasting,* **15,** 416–431.
Rotunno, R., J. B. Klemp, and M. L. Weisman, 1988: A theory for strong, long-lived squall lines. *J. Atmos. Sci.,* **45,** 463–485.
Schmidt, J. M., and W. R. Cotton, 1989: A High Plains squall line associated with severe surface winds. *J. Atmos. Sci.,* **46,** 281–302.
Skamarock, W. C., M. L. Weisman, and J. B. Klemp, 1994: Three-dimensional evolution of simulated long-lived squall lines. *J. Atmos. Sci.,* **51,** 2563–2584.
Smith, B. E., 1990: Mesoscale structure of a derecho-producing convective system: The southern Great Plains storms of 4 May 1989. Preprints, *16th Conf. on Severe Local Storms,* Kananaskis Park, AB, Canada, Amer. Meteor. Soc., 455–460.
Spoden, P. J., C. N. Jones, J. Keysor, and M. Lamb, 1998: Observations of flow structure and mesoscale circulations associated with the 5 May 1996 asymmetric derecho in the lower Ohio Valley. Preprints, *19th Conf. on Severe Local Storms,* Minneapolis, MN, Amer. Meteor. Soc., 514–517.
Trier, S. B., W. C. Skamarock, and M. A. LeMone, 1997: Structure and evolution of the 22 February 1993 TOGA COARE squall line: Organization mechanisms inferred from numerical simulation. *J. Atmos. Sci.,* **54,** 386–407.
Wakimoto, R. M., 1982: The life cycle of thunderstorm gust fronts as viewed with Doppler radar and rawinsonde data. *Mon. Wea. Rev.,* **110,** 1060–1082.
——, 2001: Convectively driven high wind events. *Severe Convective Storms, Meteor. Monogr.,* No. 50, Amer. Meteor. Soc., 255–298.
Weisman, M. L., 1993: The genesis of severe, long-lived bow echoes. *J. Atmos. Sci.,* **50,** 645–670.
——, and C. A. Davis, 1998: Mechanisms for the generation of mesoscale vortices within quasi-linear convective systems. *J. Atmos. Sci.,* **55,** 2603–2622.
Ziegler, C. L., and E. N. Rasmussen, 1998: The initiation of moist convection at the dryline: Forecasting issues from a case study perspective. *Wea. Forecasting,* **13,** 1106–1130.